LUND UNIVERSITY

Lidar system applied in atmospheric pollution monitoring

Fredriksson, K; Galle, B; Nystrom, K; Svanberg, Sune

Link to publication

Lidar system applied in atmospheric pollution monitoring

K. Fredriksson, B. Galle, K. Nyström, and S. Svanberg

A lidar system, incorporating tunable dye lasers and a 25-cm diam Newtonian telescope, has been constructed and applied in atmospheric pollution monitoring. The system, which is fully controlled by a specially designed microcomputer, has been used in several field tests, where stack effluents as well as the ambient air have been monitored. Results from particle, NO_2, and SO_2 measurements are discussed.

Introduction

Remote sensing methods are becoming increasingly important for monitoring the state of the earth's atmosphere. By using laser techniques, atmospheric pollution can be studied in long-path absorption or atmospheric backscattering experiments. Of the many reviews that have been written on this topic, we would like especially to mention the 1976 monograph edited by Hinkley.[1] The laser radar or lidar approach offers particular advantages because of its single-ended nature and great flexibility. Pulsed laser light is transmitted into the atmosphere, and light backscattered from particles and aerosols is collected by an optical telescope and analyzed. Apart from particle content information, knowledge of the 3-D distribution of certain molecular pollutants can be obtained using the so-called dial (differential absorption lidar) technique. Here the particle backscattering is measured for two wavelengths, where the gas to be investigated absorbs strongly and weakly, respectively. This technique was pioneered by Schotland,[2] and early laser work was performed by Rothe et al.,[3] Grant et al.,[4] and others. In 1975 we started a program of atmospheric laser probing at this department. In this paper we describe the lidar system that we constructed and discuss results from several field tests, where particles, NO_2, and SO_2 were studied. Our system incorporates tunable dye lasers and uses a Newtonian telescope. A specially designed microcomputer fully controls the measurement procedure.

For a lidar system, information from a distance R is obtained at a time delay $t = 2R/c$ after the transmission of the laser pulse, traveling with the velocity of light c. The power $P_\lambda(R, \Delta R)$ received from the interval ΔR at the range R is given by the general lidar equation:

$$P_\lambda(R, \Delta R) = CW\sigma_b N(R)\frac{\Delta R}{R^2}$$

$$\exp\left\{-2\int_0^R [\sigma(\lambda)n(r) + \sigma_a N(r)]dr\right\}, \quad (1)$$

where W is the transmitted pulse power, and $N(R)$ is the concentration of scatterers with the backscattering cross section σ_b. The exponential describes the attenuation of the beam and the backscattered light. The attenuation is caused by absorption due to molecules of concentration $n(r)$ and absorption cross section $\sigma(\lambda)$ and scattering and absorption due to particles of concentration $N(r)$ and cross section σ_a. C is a system constant. In particle studies it is sometimes a reasonable approximation to neglect the absorption term. If, then, σ_b is assumed to be a constant, $N(R)$ can be directly mapped in three dimensions. As the value of σ_b is not generally known, only relative concentration distributions are usually obtained. In dial measurements of gas concentrations, use is made of the fact that wavelength regions can be found where $\sigma(\lambda)$ strongly changes for a small wavelength change, while σ_b and σ_a stay approximately constant. In these conditions, the evaluation of the experimental data is quite simple. If more than one gas absorbs in the wavelength region of interest, a summation must be performed in the exponential factor.

Lidar System

The lidar system used in these measurements is schematically shown in Fig. 1. The system includes three different pulsed lasers, a Newtonian telescope, and detection, controlling, and processing electronics.

Fig. 1. Schematic diagram of the lidar system.

This unit has a memory consisting of 4096 24-bit words that may be divided into sixteen or fewer parts. The maximum transient frequency is 400 Hz. The number of transients to be averaged, the laser wavelength setting, the telescope steering, and the readout on a strip-chart recorder are controlled by the microcomputer, which also can do arithmetic operations. Thus the measuring cycle can be fully automatized. The measurement process is monitored on oscilloscopes via continuous readouts of the individual and the averaged lidar signals. In some lidar measurements a boxcar averager is used instead of the transient digitizer. In this case the lidar signals from only one or two distances are studied at each laser pulse. In some measurement modes a chopper is used to block every second or ninth shot from the laser. Then rf interference, caused by the nitrogen laser, and the background signal level are subtracted from the lidar signals. The lidar system is described in more detail in an institute report.[5] In measurements over the city of Goteborg, the system has been placed in a suitably located laboratory within the Physics Department; during field tests it was housed in a small truck.

Measurements of Particles

We have used the lidar system in several studies of particle emissions from industrial smoke stacks. Measurements of relative particle distributions are easy to perform using elastically backscattered light and neglecting weak effects of beam attenuation. To obtain good spatial resolution it is important to use a laser of short pulse length. Normally we have used the 10-nsec UV pulses from the N_2 laser. In Fig. 2 the result of a vertical scan downwind an industrial area is shown.

The choice of laser transmitter is dependent on the measuring technique employed. A 400-kW nitrogen laser with 10-nsec pulses at 337 nm is used in measurements of particles and aerosols. The repetition rate is 10–50 pulses/sec. In NO_2 measurements, a dye laser pumped by the nitrogen laser is used. The dyes Coumarin 45 or Coumarin 47, giving about 0.5 mJ in 5-nsec pulses in the 440–480-nm region, are used to produce light of suitable wavelengths in the NO_2 absorption band. Wavelengths around 300 nm in the UV absorption band of SO_2 are obtained with a frequency-doubled flashlamp pumped dye laser as 1-μsec pulses with the energy 0.4 mJ at a repetition rate of 10–25 Hz. The wavelength setting of the dye lasers is made by stepper motors.

The Newtonian telescope has a 25-cm mirror with a focal length of 100 cm and is constructed with a mount for vertical and horizontal turnings. The turnings are effected with computer-controlled motors. The laser beam is transmitted to an output mirror (placed inside the telescope) by means of first-surface aluminum mirrors in such a way that the transmitted laser beam and the optical axis of the telescope are almost coaxial at every positioning of the system. Alternatively, the flashlamp pumped dye laser can be placed on a table rotating together with the telescope. The field of view of the telescope normally corresponds to 2 mrad to match the divergence of the dye lasers. Interference filters, 5–10 nm broad with a transmission of 35–55%, are used to suppress the background skylight. Another variation is that the system may be used with a 500-mm Bausch & Lomb grating monochromator.

The spectrally filtered lidar signal is detected by an EMI 9558 QB PMT. A fast transient digitizer, Biomation 8100 with 2048 8-bit channels, is used to convert the signal to time-resolved digital data. The data are transferred to a microcomputer for signal averaging.
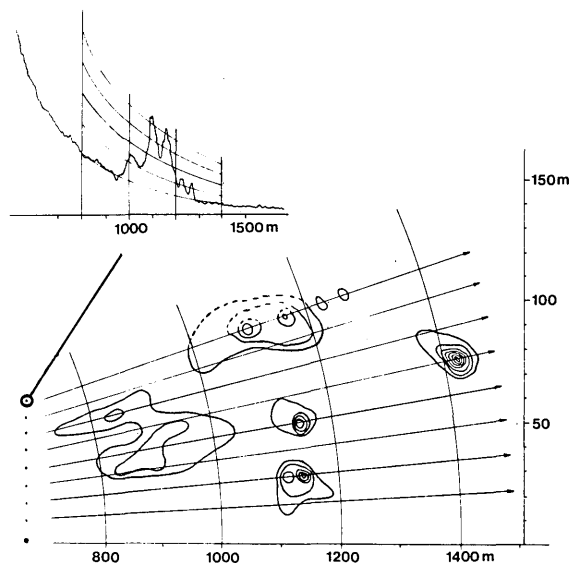

Fig. 2. Relative particle distribution downwind an industrial area, obtained in a vertical lidar scan employing a nitrogen laser. An experimental curve illustrating the evaluation procedure is included.
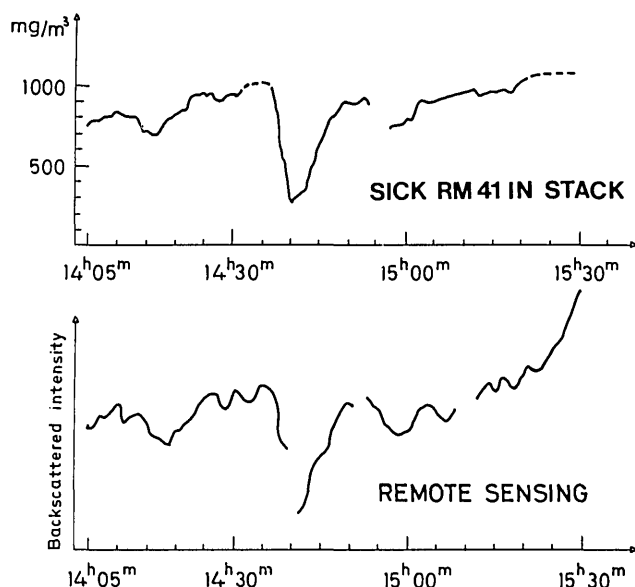
Fig. 3. Comparison between lidar and in-stack measurements of particle concentrations. The lidar curve features the amplitude of the elastic plume echo as recorded at 220-m distance. The curve deviations are discussed in the text. The in-stack instrument measured the attenuation of white light across the plume diameter. This instrument was calibrated against sampling measurements.

The lidar system was placed about 1 km away from the area to be investigated. In the illustration, an example of a recorded lidar curve is shown, featuring several echo structures from spreading plumes. The $1/R^2$ curve from the background particle concentration is clearly seen. In addition, $1/R^2$ curves corresponding to higher concentrations are indicated. The particle distribution diagram given in the illustration was constructed by locating the intersections between such equidistant curves and the actual backscattering profile for different elevation angles. We have used similar techniques to map the extensions of isolated spreading plumes. This can readily be done even for plumes invisible to the naked eye. Plume mapping techniques have been discussed, e.g., by Uthe and Wilson.[6]

If absolute particle loads in stack effluents are to be measured, the lidar system should be pointed to the plume as close to the mouth of the stack as possible. This approach avoids both influences due to wind and due to condensing water droplets. Because of the complexity of the Mie scattering theory and the lack of detailed information on particle characteristics, it is normally necessary to provide an in-stack calibration. If the particle concentration is not too high, the amplitude of the plume echo can be used in the evaluation procedure. For dense plumes it is preferable to measure the beam attenuation by the plume, measured in the light backscattered from the air before and behind the plume ("plume opacity").[7] In Fig. 3 a particle measurement is illustrated. The remote sensing curve displays the amplitude of the plume echo vs time. The measurement was performed using the boxcar averager,

set to sample the intensity at a delay time corresponding to the light round-trip time to the plume, in the actual case situated at 220-m distance from the lidar system. Comparison is made with the in-stack curve obtained with a calibrated recording instrument. The parts lacking on each curve correspond to zero calibration intervals. A good correlation between the curves was found except during the situations when the in-stack instrument was out of range. From the curves the proper calibration for the particular type of smoke (from an iron-alloy melting furnace) could be established.

Measurements of NO₂

In measurements of gaseous pollutants, the dial technique is normally employed. As mentioned above, this technique is based on the difference in absorption cross section of a certain molecular gas at two or more close lying wavelengths. At normal atmospheric conditions the backscattering and the absorption of particles and aerosols are slowly varying functions of the wavelength. Thus, a fast wavelength dependence in the lidar Eq. (1) will be solely due to absorbing gases, making the exponential factor change. The system constant C may also have a fast wavelength dependence, e.g., from Fabry-Perot effects in the transmitting and receiving optics, but this is automatically taken care of by the evaluation procedure. The dial equation is obtained from Eq. (1) as

$$\frac{P_{\lambda_1}(R)}{P_{\lambda_2}(R)} = C' \cdot \exp\left\{-2\int_0^R [\sigma(\lambda_1) - \sigma(\lambda_2)]n(r)dr\right\}, \qquad (2)$$

where C' is a new constant, and it is assumed that only one atmospheric gas has a differential absorption at the two wavelengths λ_1 and λ_2. If $\sigma(\lambda_1)$ is larger than $\sigma(\lambda_2)$, it follows from Eq. (2) that the dial signal

$$P_{\lambda_1}(R)/P_{\lambda_2}(R)$$

will decrease with the distance R in the presence of the studied gas.

We have measured NO₂ concentrations with the dial technique in the 440–460-nm wavelength region. The cross-section values used in the calculations are those given by Grant et al.,[4] with wavelength extensions made in absorption measurements in our laboratory fitted to these values. Deviations from these, as obtained in laboratory measurements by Woods and Jolliffe,[8] are within the uncertainty limits. Possible corrections at high temperatures in smokestack plumes have not been considered in these measurements.

Our first measurements on gaseous pollutants concerned NO₂ concentrations in smokestack plumes of an oil refinery. The lidar system was located at a distance of 2 km from the stack studied. In Fig. 4 a measurement is shown in which the lidar was directed just above the top of the smokestack. The backscattered intensity from the atmosphere surrounding the plume, measured for two different wavelengths, is displayed. The lidar signal of the plume is far beyond scale and is cutoff in the figure. This measurement implies an integrated concentration of 190 ± 50 mg/m³ · m, which equals 30 ± 10 mg/m³ as an average in the plume. The uncer-
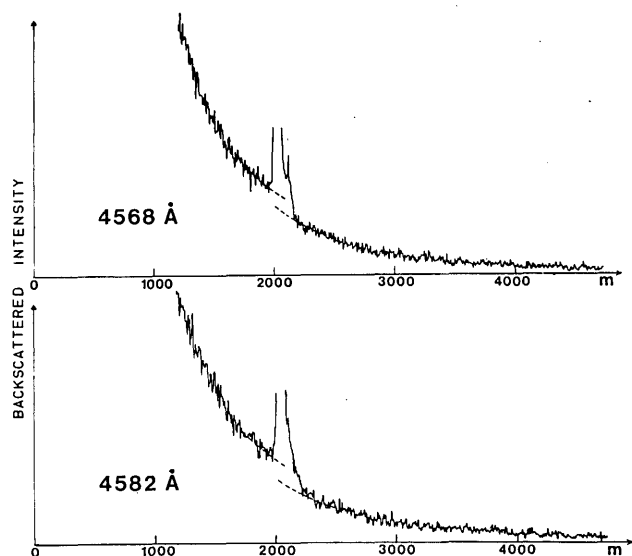
Fig. 4. Measurement of the NO_2 content in the plume from an oil-refinery stack situated 2 km from the remote sensing system. Two lidar curves for two close-lying wavelengths with different absorption cross sections are shown. A NO_2 concentration of 30 ± 10 mg/m^3 through the 6-m thick plume is inferred.
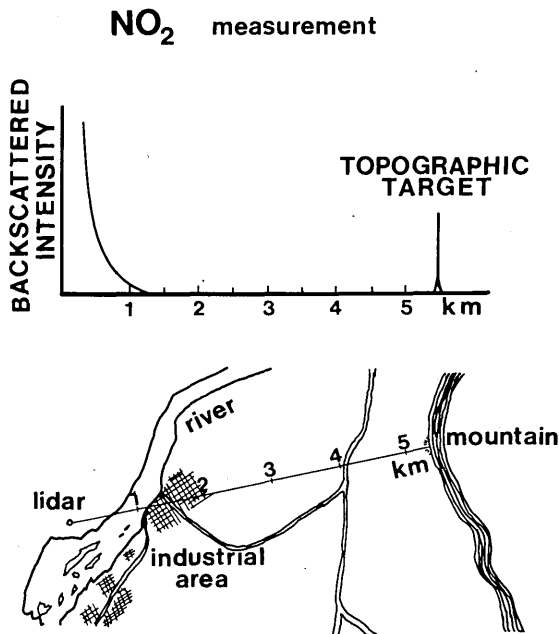

Fig. 5. The lidar curve shows topographic-target echo as well as atmospheric backscattering. Measurements at two wavelengths, 446.5 nm and 448.5 nm, yielded a mean NO_2 concentration of 2 ± 2 ppb over the 0.5–5.5-km range interval.

tainty limits of these values are determined by the statistical noise in the measurement curves. The upper limit of the concentration is further inferred by the individual attenuation in each of the two curves. The concentration was found to be much below this value during most of the measuring period.

Plumes from an oil-burning power plant were also studied, and the NO_2 contents were found to be below

30 mg/m^3 · m at the top of the smokestack. Measurements of exhausts from än aeroengine manufacturer during tests of jet engines implied very high NO_2 contents; values up to 900 mg/m^3 · m were obtained. These NO_2 measurements were performed at a range of 1 km. NO_2 concentrations in the ambient air have been measured in different types of areas. Tens of parts per billion have been recorded in the city of Goteborg. When average concentrations over large distances are to be measured, one may use some distant topographic target instead of the atmosphere for the backscattering of the laser beam. Such a measurement is shown in Fig. 5, where a mountain at a distance of 5.5 km is used as the backscattering target. This measurement yields an average concentration of 2 ± 2-ppb NO_2.

Measurements of SO_2

In the dial measurements of SO_2, wavelengths in the absorption band around 300 nm are used. The absorption cross-section values used in our evaluations are those given by Thompson et al.[9] Corrections to these values at high temperatures, as discussed by Jolliffe and Woods[10] and Exton,[11] are made in measurements of smokestack plumes. Wavelength calibration was made using absorption cells containing SO_2.

In addition to dial measurements at two wavelengths, a modified type of dial technique was applied when measuring high SO_2 concentrations in smokestack plumes. Then the attenuated lidar signal as measured through the plume is compared with the signal obtained in a direction beside the plume. Only one laser wavelength, with rather low SO_2 cross section, is used, and thus the method is useful only when the attenuation caused by particles is negligible. This technique is preferable at high concentrations, since the laser light at the strongly absorbed wavelength is then almost completely blocked by the gas. Alternatively, one may use the ordinary dial technique in the region of weaker absorption around 315 nm.

Measurements of the SO_2 contents in plumes from an oil-burning power station were made. Concentrations in the 300–550-ppm range were obtained using the modified dial technique. In Fig. 6 such a measurement of SO_2 is shown. The registration curve displays the result obtained from a division of the lidar recordings in a direction through the plume and beside it, respectively. Compared with Eq. (2), this equals a situation where $\sigma(\lambda_2)$ is zero. The 1-μsec pulse length of the flashlamp pumped dye laser reduces the spatial resolution; therefore, the lidar plume echo in Fig. 6 is rather broad. Measurements of outlets from an iron-alloy plant and from other pollution sources were also made as well as studies of the spreading of SO_2 plumes.

We have also performed measurements of ambient SO_2 concentrations in urban as well as in industrial areas. Figure 7 shows a measurement of the lidar signal from the atmosphere at a distance of 1 km at six different wavelengths. Each value has been normalized to the short-range atmospheric lidar signal. The values

$\frac{P(R)}{\overline{P}(R)}$

ELASTIC
PLUME ECHO

SO$_2$ ABS.

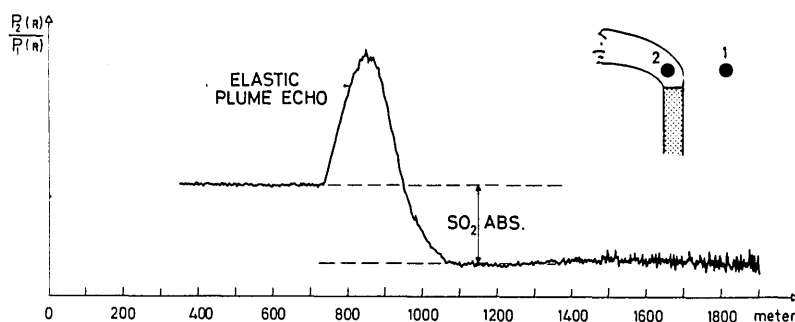0   200   400   600   800   1000   1200   1400   1600   1800   meter

Fig. 6.   Lidar measurement of SO$_2$ emission from an oil-burning power station.   Two lidar curves, measured through and beside the smoke plume, have been divided, displaying the smoke-particle scattering as well as the attenuation due to SO$_2$.   A SO$_2$ concentration of 760 ± 150 mg/m^3 was inferred across the 4.5-m diam plume.

SO$_2$ dial measurement 0 – 1 km

Normalized backscattered intensity

r.p.

o10 ppb
o*
o25 ppb
o40 ppb

* experimental
o theoretical
r.p. reference point
for theoretical
values
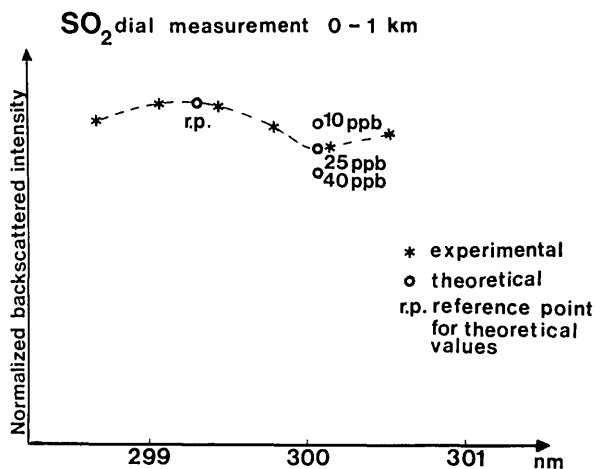
299   300   301   nm

Fig. 7.   Normalized atmospheric backscattering from a distance of 1 km measured at six wavelengths around 300 nm.   The reference point and the theoretical values are located at the minimum and maximum absorption wavelengths as obtained in laboratory spectra.   A mean concentration value of 25 ± 8 ppb was obtained.

show the time of the individual measurements. Comparison is made with the day average value obtained by the local Public Health Board with a conventional chemical measuring method.   As can be seen, the remote sensing results are fully compatible with the reference value.

Conclusions

The lidar system described in this paper has proved efficient and useful for atmospheric probing.   Within its basic constraints it has been gradually refined as a result of the experience gained in an extended field-test program.   A more detailed account of the different types of measurements discussed is given in Refs. 5 and 12–15.   Based on this work, we are now developing a fully mobile dedicated lidar facility for the Swedish Space Corporation.   The system, housed in a 6-m covered truck, is based on a Nd:YAG pumped dye laser and
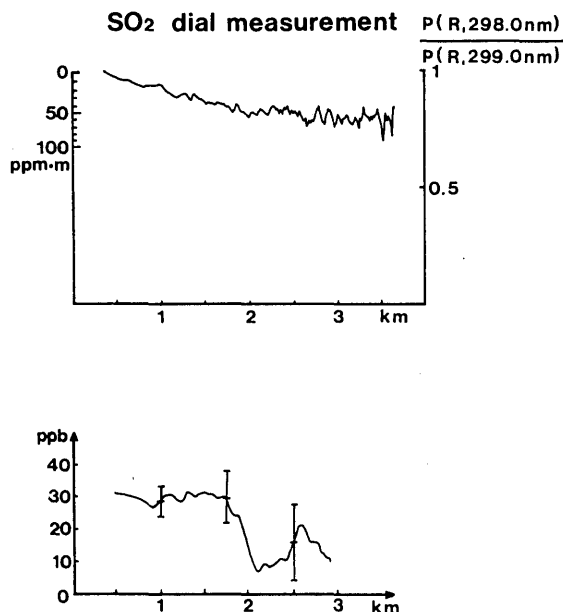

SO$_2$ dial measurement $\frac{P(R, 298.0 \text{nm})}{P(R, 299.0 \text{nm})}$

0
50
100
ppm·m

1

0.5

1   2   3   km

ppb
40
30
20
10
0

1   2   3   km

Fig. 8.   Dial curve for range resolved SO$_2$ concentration determination, based on measurements at 298.0 nm and 299.3 nm.   In the lower part of the figure, the concentration, averaged over a 500-m interval continuously swept with the distance, is shown.   The bars in the figure indicate the uncertainty limits as inferred from the dial curve influenced by statistical photon noise and atmospheric turbulence.
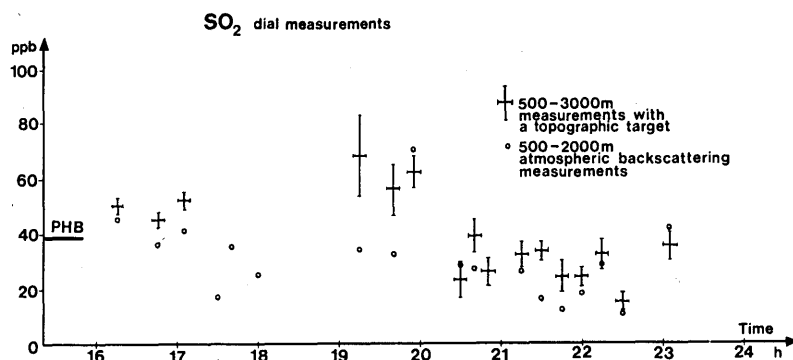
agree with the absorption feature of SO$_2$, and an average concentration of 25 ± 8 ppb is implied from this measurement.

A typical two-wavelength dial measurement of SO$_2$ in the ambient air is shown in Fig. 8.   The upper curve displays the dial signal according to Eq. (2), and the vertical scale expresses the SO$_2$ concentration as integrated from 500 m.   The lower curve shows the concentration obtained when the dial signal is evaluated over 500-m intervals.   This measurement was made in an area where the background level is rather low and where the atmosphere up to a distance of 2 km is polluted from an industrial area.

Several studies of the SO$_2$ pollution situation in Goteborg were made.   A measurement of the time-varying concentration over a period of 7 h is shown in Fig. 9.   Evaluations of the backscattered return from the atmosphere at 2 km as well as from a topographic target at a distance of 3 km are shown in the figure.   The vertical bars in the figure indicate the estimated maximal errors in the measurements; the horizontal bars

Fig. 9. Time variation of the SO_2 concentration over the city of Goteborg. The average concentration over a distance of 3 km, as determined in dial measurements against a topographic target, is shown with indications of the time periods of measurement and the estimated maximal error. In addition, mean values over a distance of 2 km are given by rings, as obtained in dial measurements using atmospheric backscattering. The day average value as measured by the local Public Health Board (PHB) with conventional chemical methods is also given. This value was obtained at a point along the measurement path.

a fixed vertical 30-cm telescope. A beam-steering plane mirror plus the transmitter and receiver electronics are controlled by a minicomputer. The mobile system will be operated by the Swedish Environmental Protection Board for monitoring particles, NO_2, SO_2, and O_3. Future extensions to CO, CH_4, and HCl are foreseen. A system of this kind is also useful for hydrospheric probing as has been demonstrated, e.g., in this laboratory.[16-18] Thus the lidar concept has important implications to environmental diagnostics.

References

1. E. D. Hinkley, Ed., *Laser Monitoring of the Atmosphere, Topics in Applied Physics, Vol. 14* (Springer, Berlin, 1976).
2. R. M. Schotland, in *Proceedings of the Third Symposium on Remote Sensing of the Environment* (University of Michigan, Ann Arbor, 1964).
3. K. W. Rothe, U. Brinkmann, and H. Walther, Appl. Phys. 3, 116 (1974); 4, 181 (1975).
4. W. B. Grant, R. D. Hake, Jr., E. M. Liston, R. C. Robbins, and E. K. Proctor, Jr., Appl. Phys. Lett. 24, 550 (1974); W. B. Grant and R. D. Hake, Jr., J. Appl. Phys. 46, 3019 (1975).
5. K. Fredriksson, B. Galle, A. Linder, K. Nyström, and S. Svanberg, "Laser Radar Measurements of Air Pollutants at an Oil-Burning Power Station," Goteborg Institute of Physics Report GIPR-150 (1977).
6. E. E. Uthe and W. E. Wilson, in *Proceedings of the Fourth Joint Conference on Sensing of Environmental Pollutants, 1977* (American Chemical Society, Washington, D.C., 1978).
7. C. S. Cook, G. W. Bethke, and W. D. Conner, Appl. Opt. 11, 1752 (1972).
8. P. T. Woods and B. W. Jolliffe, Opt. Laser Technol. 10, 25 (1978).
9. R. T. Thompson, Jr., J. M. Hoell, and W. R. Wade, J. Appl. Phys. 46, 3040 (1975).
10. B. W. Jolliffe and P. T. Woods, private communication.
11. R. J. Exton, *NASA Technical Paper 1014* (U.S. PO, Washington, D.C., 1977).
12. K. Fredriksson, I. Lindgren, S. Svanberg, and G. Weibull, "Measurements of the Emission from Industrial Smokestacks Using Laser-Radar Techniques," Goteborg Institute of Physics Report GIPR-121 (1976).
13. K. Fredriksson, I. Lindgren, K. Nyström, and S. Svanberg, "Field Test of a Lidar System for the Detection of Atmospheric Pollutants," Goteborg Institute of Physics Report GIPR-134 (1976).
14. K. Fredriksson, A. Linder, I. Lindgren, K. Nyström, and S. Svanberg, "Some Preliminary Measurements of SO_2 Concentrations Using a Differential Absorption Lidar System," Goteborg Institute of Physics Report GIPR-136 (1977).
15. K. Fredriksson, B. Galle, K. Nyström, and S. Svanberg, "Measurements of Air Pollutants in the Trollhättan Area Using Lidar Techniques," Goteborg Institute of Physics Report GIPR-171 (1978).
16. L. Celander, K. Fredriksson, B. Galle, and S. Svanberg, "Investigation of Laser-Induced Fluorescence with Applications to Remote Sensing of Environmental Parameters," Goteborg Institute of Physics Report GIPR-149 (1978).
17. K. Fredriksson, B. Galle, K. Nyström, S. Svanberg, and B. Öström, "Underwater Laser-Radar Experiments for Bathymetry and Fish-School Detection," Goteborg Institute of Physics Report GIPR-162 (1978).
18. K. Fredriksson, B. Galle, K. Nyström, S. Svanberg, and B. Öström, Medd. Havsfiskelab. Lysekil No. 245 (1979).